

## Supplementary information of article

### Water migration through fat-based semi solid heterogeneous materials

H. de Cagny<sup>1,2\*</sup>, J. C. Rouwhorst<sup>1\*</sup>, L. Arnaudov<sup>2</sup>, S. Stoyanov<sup>2</sup>, T.B.J. Blijdenstein<sup>2</sup>, and P. Schall<sup>1</sup>

<sup>1</sup>*Van der Waals-Zeeman Instituut, Institute of Physics, University of Amsterdam, 1090 GL Amsterdam*

<sup>2</sup>*Unilever Foods Innovation Centre, Bronland 14, 6708 WH, Wageningen*

\*These authors contributed equally

#### *Sample preparation*

The samples consist of heterogeneous mixtures of a continuous fat phase with solid inclusion (salt particles) trapped in it. Palm oil stearin, POs53, was used for the fat continuous phase. The stearin was purchased from Sime d'Arby Unimills B.V. (Zwijndrecht, the Netherlands) and was separated from the palm oil by fractionation. The fatty acid composition is measured by 2-position-FAME (Fatty Acid Methyl Ester gas chromatography) (1) and AgCl column (2) (3) separation and results can be found in tables I and II. Furthermore, the fat was characterized by a melting trajectory, indicated as an N-line which gives the weight fraction of solid fat (N) at a given temperature. For this specific fat,  $N_{10}= 0.85$ ,  $N_{20}= 0.69$ ,  $N_{30}= 0.45$ ,  $N_{40}= 0.28$ , as measured by a standard NMR-method (4).

Fatty acid	Fatty acid content (Norm. %)
C 6:0	-
C 8:0	-
C10:0	-
C11:0	-
C12:0	1,3
C13:0	-
C14:0	1,2
C14:1	-
C15:0	<0,1
C15:1	-
C16:0	38.4
C16:1	0.1
C17:0	<0.1
C17:1	<0.1
C18:0	2.4
C18:1	42.5
C18:2	11.9
C18:3	0.6
C20:0	0.2
C22:0	-
C24:0	<0.1
C24:1+C22:6	<0.1
Unknowns	1.03

**Table I Fatty acid composition of POs53 used in this study as measured by 2POS Fame.**

The salt used was micro salt obtained from Akzo Nobel (Deventer, the Netherlands). The average size of the micro salt was characterized with a Morphologi G3S and the average size measured was 500 $\mu$ m. The precise composition of the fat and the size distribution of the salt can be found in the Table II.

To prepare heterogeneous samples with the desired volume fraction, it is necessary to know the density of the fat phase. The density was measured with a densitometer DMA 45 at various temperatures. At ambient temperature, the density is found to be equal to 0.939g/ml. The samples are prepared by initially melting the fat flakes at 90 °C. The fat is then poured on aluminum foils where they crystallize while cooling down, forming sheets of fat crystals. The salt is poured in a kitchen mixer (Kenwood), equipped with a K-beater type of geometry, and gently mixed with the water during two minutes. The fat is then added, and the slurry is mixed until the formation of a compact and solid paste. The mixing is then stopped, to prevent overworking and aeration of the paste. The slurry necessary to prepare cubes of dimension 23x28x11.5mm is then individually weighed for each cube. The resulting amount is poured in a mold made of 20 rectangular holes of dimension (23mmx28mm). The slurry is then compressed by a universal testing machine (Instron 5567) until the samples reach the desired height. After compression, the cubes are stored for 4 weeks at ambient temperature so that the crystallization process can finish. For each salt volume fraction  $\phi_{NaCl}$ , two batches of 20 cubes are prepared.

$\phi_{NaCl}$	$\phi_{H_2O}$	$\phi_{fat}$	$w_{NaCl}$	$w_{H_2O}$	$w_{fat}$	$\phi_{NaCl\ solid}$
0.5	0	0.5	0.698	0	0.302	0.5
0.5	0.01	0.49	0.698	0.006	0.296	0.498
0.5	0.02	0.48	0.698	0.012	0.290	0.497
0.5	0.03	0.47	0.667	0.019	0.284	0.495
0.5	0.04	0.46	0.697	0.026	0.279	0.493
0.5	0.05	0.45	0.697	0.032	0.271	0.492
0.5	0.07	0.43	0.696	0.045	0.259	0.488
0.5	0.1	0.4	0.695	0.064	0.240	0.483
0.5	0.13	0.37	0.694	0.083	0.223	0.478

**Table II Volume fraction ( $\phi$ ), mass fraction ( $w$ ) of the three phases samples.** We also added the theoretical amount of solid salt  $\phi_{NaCl}$  that did not dissolve in water. The density of the fat was found to be  $\rho_{fat} = 970kg.m^{-3}$ , and the density of the sodium chloride is  $\rho_{NaCl} = 2170 kg m^{-3}$ . The theoretical amount was calculated using the maximum solubility of NaCl in water at 25 degrees Celsius (357mg.mL<sup>-1</sup>) (5)

### SEM-EDX measurements

Scanning Electron Microscopy (SEM) was used to gain high resolution information about the microstructure of the samples. SEM visualizes details of surfaces. To observe the internal structure the sample has to be fractured or planed and in this particular study samples were planed in order to provide a smooth surface for EDX analysis. High resolution SEM requires a high vacuum, which does not allow wet samples. Also, oil/fat containing products need to be cryo-fixed to get good imaging quality and no influence of oil leakage (in vacuum sample covers with an oil layer). This was circumvented by freezing the samples in slush liquid nitrogen (LN2).

Two types of signals produced by SEM including back-scattered electrons (BSE) and characteristic X-rays were used. The BSE signal is strongly related to the atomic number (Z) of the compounds present (BSE yields images with areas with different grey levels, which gives

locations with different mass densities). Characteristic X-Rays are emitted when the electron beam removes an inner shell electron from the molecule, causing a higher energy electron to fill the shell and release energy. These characteristic X-rays are used to identify the composition and measure the abundance of elements in the sample. The detection of X-rays is performed by an Energy Dispersive X-ray Detector (EDX). The full sample pretreatment protocol for the SEM experiments is as follows:

A piece of  $\sim 4\text{mm} \times 4\text{mm} \times 6\text{mm}$  is cut out of the sample and put into a 4 mm sample cup with tissue-tek and frozen by putting the cup in dry ice. The cup is placed into the cryo-ultramicrotome (Leica Ultracut UCT EM FCS) and cryo-planed with a slice thickness of 100 nm and a speed of 60 mm/sec using a glass knife at  $-110^\circ\text{C}$  to create sufficient and sufficient smooth surface. Subsequently, the sample is stored one night in liquid nitrogen container to obtain a clean surface (debris free) and a second Cryo-planing with section thickness of a few nm and a speed of 2 mm/sec using a diamond knife (Diatome histo cryo 8 mm) is performed at  $-110^\circ\text{C}$  to enable complete smoothness as indicated by visual mirroring of the surface. After planning, the sample cup is mounted onto a holder and transferred into a Gatan Alto2500 preparation chamber at  $-125^\circ\text{C}$ . Then, the temperature of the sample is increased to  $-90^\circ\text{C}$  during 3 min (to remove a thin layer of water by sublimation) and sputter coating with platinum is performed for 20 sec at  $-125^\circ\text{C}$  (10 mA) for a better SEM contrast and to prevent charging by the electron beam. Finally, the coated sample is transferred to the Zeiss Auriga field-emission SEM at  $-125^\circ\text{C}$  and SEM images (SE / BSE / Inlens) are acquired at accelerating voltages of 3 to 10kV and EDX maps are recorded at 10kV (EDX Oxford 80mm<sup>2</sup>).

### *Conductivity measurements*

The conductivity of the samples is measured with a TROTEC BM18 hygrometer, which is designed to measure humidity in woods, based on their conductivity. To convert the hygrometer readings back to conductivities, we calibrated the device using salt solutions with varying amount of dissolved salt. From the amount of dissolved salt, we computed the expected conductivity. The calibration curve is shown in Fig. S1. The data indicates a linear relationship between the hygrometer reading and the conductivity. Contaminants like carbon dioxide (which adsorbs at the cell walls) can affect the conductivity measurement; however, as the data indicates a closely linear relationship, we conclude that their effect is small.

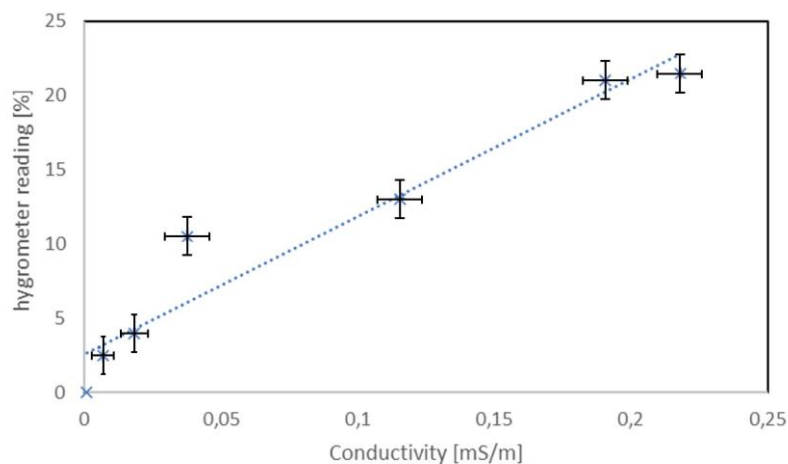


**Fig. S1 Conductivity calibration**

Hygrometer reading versus conductivity of the NaCl solutions, as determined from the amount of dissolved salt. The data indicates a roughly linear relation. The error bars are variances of the hygrometer reading over several attempts, and estimated uncertainty in the conductivity value determined from the dissolved salt.

### Simulations

To obtain insight into the formation of percolating water networks, we perform Monte Carlo simulations with randomly placed, non-overlapping spherical inclusions, to which we add a shell of thickness  $t$  to model the water absorption. The sample dimensions, inclusion concentration and size distribution are chosen to match the experimental conditions, i.e. salt inclusion concentration and measured size distribution. Shells of varying thickness  $t$  are added around the particles to mimic the water adsorption and wetting layer around the salt inclusions. We then compute the distance between the centers of the inclusions, and test for the condition that the surfaces are at a distance closer than  $t$ , the water layers thickness. The inclusions' center to center distance corresponds to  $R_1 + R_2 + d_{\text{intersurface}}$ , where  $R_1$ ,  $R_2$  are the radii of the 2 particles we test, and  $d_{\text{intersurface}}$  represents the distance between surfaces, see Fig. S2. Effectively the simulation tests for the condition that  $d_{\text{intersurface}} < 2t$ . When this condition is satisfied, the water layers of the inclusions overlap, connecting them into a cluster. Strictly, a cluster is identified as a group of particles that satisfy 2 conditions: Firstly, every particle is connected to any other particle of the same cluster. Secondly, any particle in the cluster is not connected to a particle that forms part of another cluster. Once the clusters are identified, their size, geometry and particle number can be monitored. The typical distance between particle surfaces as a function of the system volume fraction is shown in Fig. S3. It can be observed that the greatest change in the typical distance between particles is at lower volume fractions.

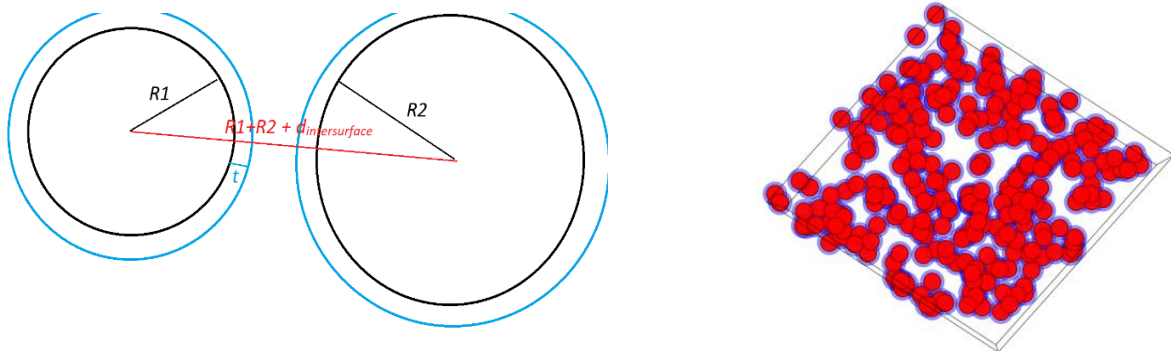


**Figure S2 Schematic of the simulation principle.** (left) When the center-to-center distance is smaller than  $R_1 + R_2 + 2t$ , where  $t$  is the water layer thickness, the water layers overlap. (right) Reconstruction of the simulated system showing the spherical inclusions (red dots) and their shells modelling the water layers (blue).

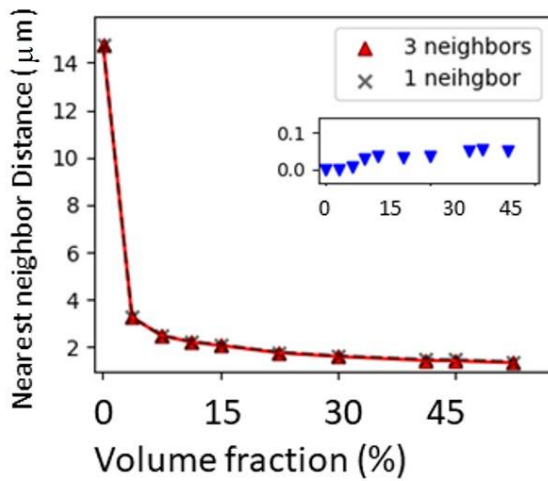


**Figure S3 Average surface-to-surface distance of nearest neighbors.** Average surface-to-surface distance of nearest neighbors computed for the closest neighbor only (crosses) and for the 3 nearest neighbors (red triangles), as a function of inclusion volume fraction. The surface-to-surface distance decreases with inclusion volume fraction, first sharply, then more gradually. Inset: Difference between the two methods (1 and 3 closest neighbors) in mm, as a function of volume fraction.

### *Rheological model*

A simple linear rheological model was used to describe the stress relaxation curves obtained in the main manuscript. This model is consisting of three standard linear solid elements in placed in parallel. Figure S4 gives a schematic representation of this model. For more details about how it can describe the relaxation curves, we refer the reader to (6)

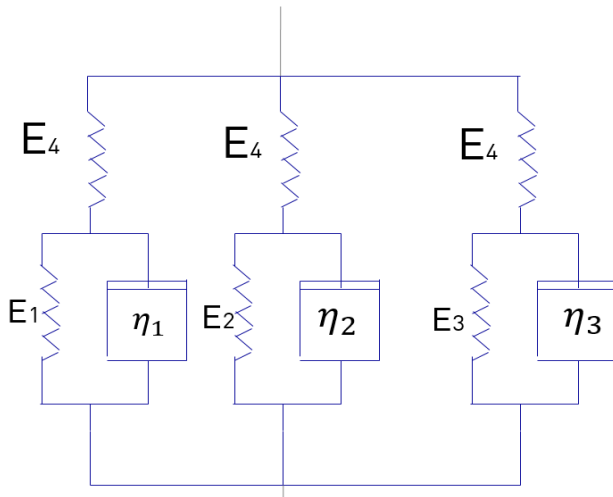


**Figure S4 Rheological model used to describe the stress relaxation curves.** The ideal solid elements are represented by springs (with an associated Young modulus  $E$ ), and the ideal viscous elements by dashpots (with viscosity  $\eta$ )

## Bibliography

1. *OFFICIAL METHODS AND RECOMMENDED PRACTICES OF THE AOCS*. 7. sl : AMER OIL CHEMIST Society, 2017. 9781630670603.
2. *Fractionation of the Triacylglycerols of Evening Primrose Oil by High-Performance Liquid Chromatography in the Silver Ion Mode*. Christie, William W. 2, sl : Wiley, 1 1 1991, *Fett Wissenschaft Technologie/Fat Science Technology*, Vol. 93, pp. 65-66. 10.1002/lipi.19910930205.
3. *Silver-phase high-performance liquid chromatography-electrospray mass spectrometry of triacylglycerols*. Schuyf, P. J.W., et al. 1-2, sl : Elsevier, 12 6 1998, *Journal of Chromatography A*, Vol. 810, pp. 53-61. 10.1016/S0021-9673(98)00277-5.
4. *Solid fat content determination by NMR*. Duynhoven, J Van en Goudappel, GJ. 95, 1999, *AOCS inform*, Vol. 10, pp. 479-484.
5. Haynes, W.m. *CRC Handbook of Chemistry and Physics*. [red.] W.M Haynes. 95. sl : CRC Press. 13:978-1-4822-0868-9.
6. *Mechanical properties of fat-based semi solid heterogeneous materials*. de Cagny, Henri, et al. 1 12 2019. 1912.00419.